

Notice: This manuscript has been authored by UT-Battelle, LLC, under Contract No. DE-AC0500OR22725 with the U.S. Department of Energy. The United States Government retains and the publisher, by accepting the article for publication, acknowledges that the United States Government retains a non-exclusive, paid-up, irrevocable, world-wide license to publish or reproduce the published form of this manuscript, or allow others to do so, for the United States Government purpose.

Supporting Information for:

Effect of Hydration on the Molecular Dynamics of Hydroxychloroquine Sulfate

Eugene Mamontov^{1,*}, Yongqiang Cheng¹, Luke L. Daemen¹, Jong K. Keum¹, Alexander I. Kolesnikov¹, Daniel Pajeroski¹, Andrey Podlesnyak¹, Anibal J. Ramirez-Cuesta¹, Matthew R. Ryder¹, Matthew B. Stone¹

¹ Neutron Scattering Division, Oak Ridge National Laboratory, Oak Ridge, TN 37831, USA

* Corresponding Author: mamontove@ornl.gov

Diffusivity of HCQS in aqueous solutions

Following subtraction of the signal from the D₂O buffer, the QENS spectra were fitted with the expression:

$$I(Q, E) = \frac{1}{\pi} \frac{\Gamma(Q)}{\Gamma(Q)^2 + E^2} \otimes R(Q, E) + (C_1(Q)E + C_2(Q)) \quad (\text{Eq. S1})$$

where $R(Q, E)$ is the experimentally measured resolution function numerically convolved with the Lorentzian quasielastic component term, and the latter term in parentheses represents a fitted linear background. The top panel of Figure S1 shows the scattering intensity and the fit components, whereas the bottom panel shows the same data as the top panel, but with the scattering and fitted intensities renormalized as $I(Q, E)/(n_{\text{Bose}}(E)+1)$, where $n_{\text{Bose}}(E) = (\exp(E/k_{\text{B}}T) - 1)^{-1}$ is Bose population factor, and k_{B} is Boltzmann's constant. At higher energy transfers, where the influence of the spectrometer resolution is relatively weak, such renormalized data approximates the imaginary part of the dynamic susceptibility, $\chi''(Q, E)$. The maxima of dynamic susceptibility correspond to the characteristic relaxation frequencies in the system, thus enabling intuitive visualization. Figure S2 shows the Q -dependence of the Lorentzian broadening describing the diffusivity in 20 mg/ml and 40 mg/ml solutions of HCQS in D₂O, fitted with a Fickian diffusion law, $\text{HWHM}(Q) = \hbar D Q^2$. Even with the D₂O buffer signal subtracted, the Q -range for the fitting is nevertheless limited to values way below the first structural maximum.

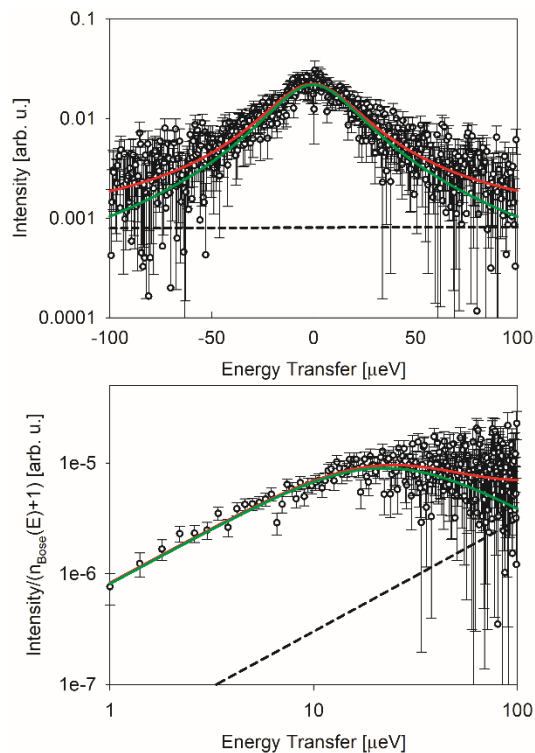


Figure S1. Top panel: QENS spectrum of 40 mg/ml solutions of HCQS in D₂O (with the D₂O buffer signal subtracted) measured using the BASIS spectrometer at 310 K at $Q = 0.9 \text{ \AA}^{-1}$. Red solid line: overall fit. Green solid line: quasielastic component of the fit. Dashed line: background component of the fit. Bottom panel: the same data as presented in the top panel, but renormalized as $I(Q,E)/(n_{\text{Bose}}(E)+1)$.

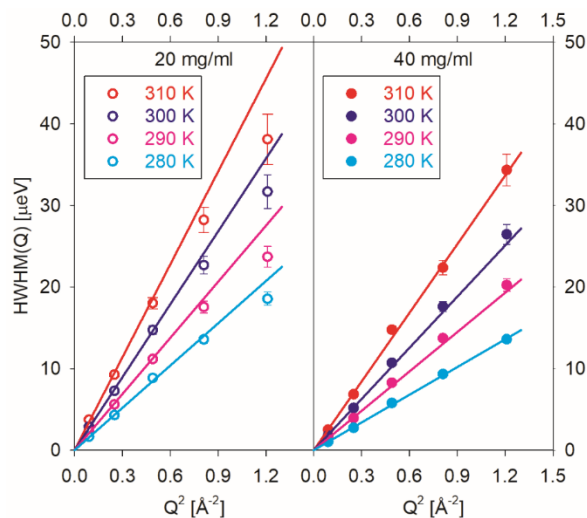


Figure S2. The Q -dependence of the Lorentzian broadening describing the diffusivity in 20 mg/ml and 40 mg/ml solutions of HCQS in D₂O measured at BASIS. Solid lines are fits to a Fickian diffusion law, $\text{HWHM}(Q) = \hbar D Q^2$.

Neutron diffraction patterns from solid samples

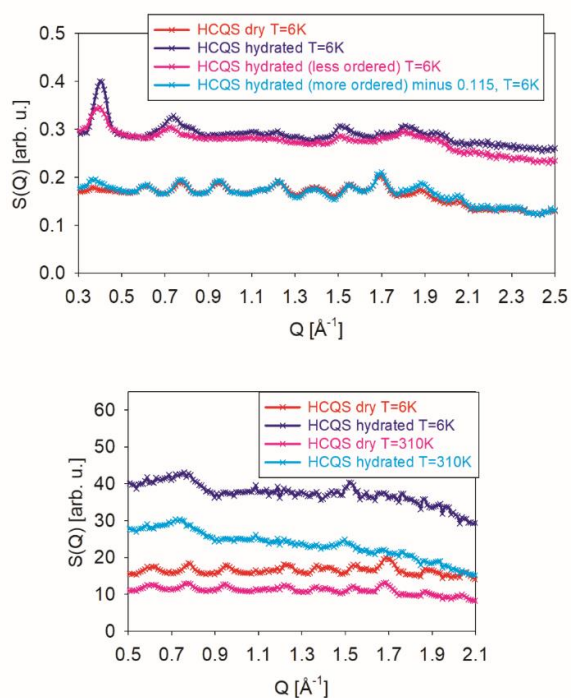


Figure S3. Neutron diffraction spectra measured at SEQUOIA with $E_i=25$ meV (top panel) and CNCS with $E_i = 3.32$ meV (bottom panel).

Mean-squared displacements (MSD) in solid samples

A diagnostic scan of the elastic scattering intensity (measuring the neutrons scattered from the sample within ± 3.7 μeV energy transfer, i.e., $\pm\text{FWHM}$ of the elastic line) was used to obtain the temperature dependence of the MSD, $\langle u^2(T) \rangle$, using the Gaussian approximation for the $Q < 1$ \AA^{-1} data, $I_{\text{elastic}}(Q,T) = I_{\text{elastic}}(Q,T_{\text{baseline}})\exp(-\langle u^2(T) \rangle Q^2)$.

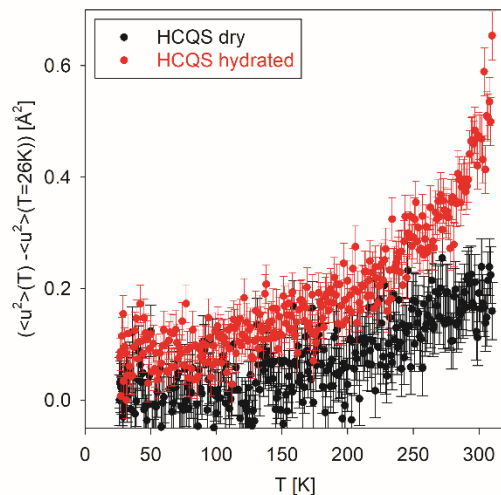


Figure S4. Temperature dependence of the mean-squared atomic displacement measured on the BASIS spectrometer for the dry and main hydrated HCQS samples. The data have been binned into steps of 0.5 K. Temperature dependent measurements were performed while cooling at a rate of 0.5 K/min.

QENS broadening in the dry and main hydrated solid samples

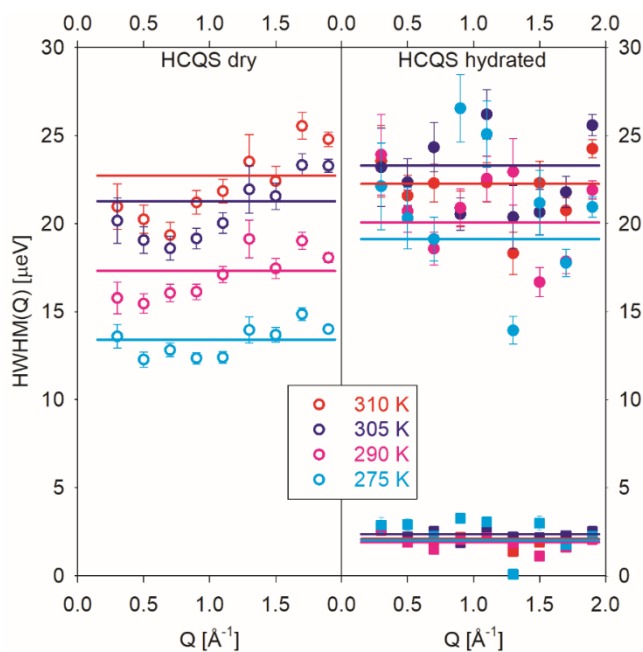


Figure S5. Q-dependence of the QENS signal HWHMs for the dry and main hydrated HCQS samples. The hydrated HCQS spectra (right panel) required two quasielastic components. Horizontal solid lines show the Q-averaged values.

Hydration water dynamics in the more ordered hydrated solid sample

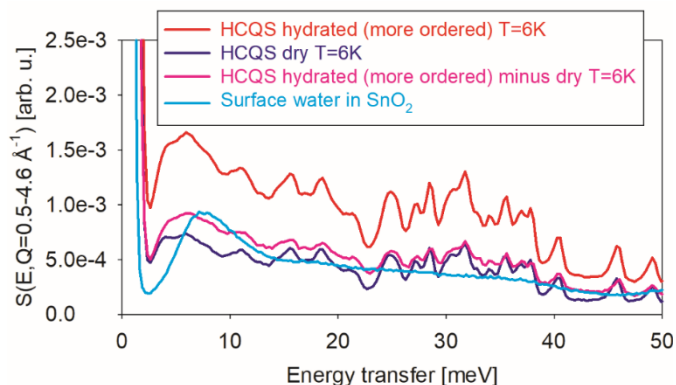


Figure S6. Q-integrated INS data collected with an incident energy of 55 meV for dry and more ordered hydrated HCQS using the SEQUOIA spectrometer. A measurement of a sample of SnO₂ with surface water is shown for comparison.

Temperature dependence of the EISF(Q) measured at BASIS for the dry and main hydrated solid samples

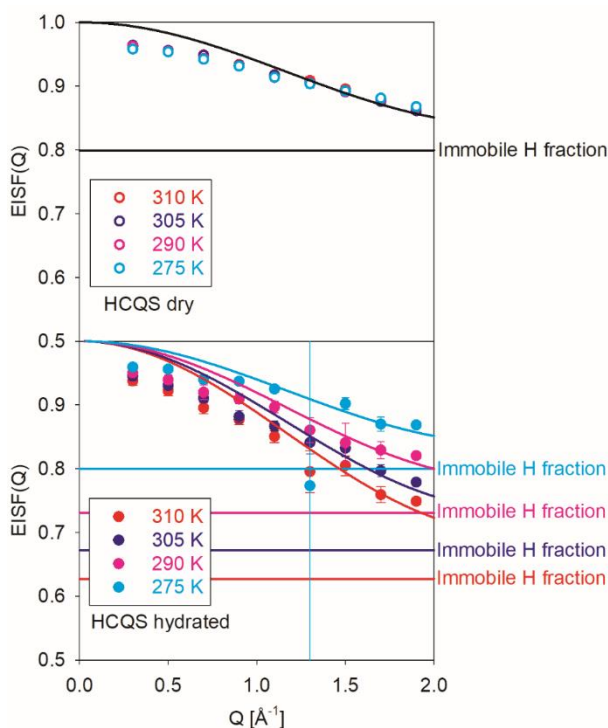


Figure S7. The temperature dependence of the elastic incoherent structure factor, EISF(Q), measured using BASIS for the dry and main hydrated HCQS samples. Solid horizontal reference lines indicate the fraction of the immobile hydrogens (parameter c in Equation 3).

Temperature dependence of the fraction of immobilized water molecules in the main hydrated sample

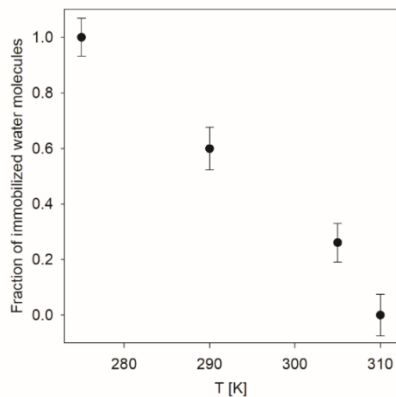


Figure S8. The temperature dependence of the fraction of the immobilized hydration water molecules in the main hydrated HCQS sample.